The 9th European Congress on Computational Methods in Applied Sciences and Engineering
ECCOMAS Congress 2024
3–7 June 2024, Lisboa, Portugal

MODELING OF STRUCTURAL COMPRESSIVE FATIGUE PROPAGATION IN CONCRETE USING THE MICROPLANE SLIDING MODEL MS1

A. Baktheer[1], S. Esfandiari[1], M. Aguilar[1], H. Becks[1], M. Classen[1], and R. Chudoba[1]

[1] Institute of Structural Concrete, RWTH Aachen University,
Mies-van-der-Rohe-Straße 1, 52074 Aachen, Germany
e-mail: abaktheer@imb.rwth-aachen.de, www.imb.rwth-aachen.de

Key words: Concrete, Fatigue, Stress redistribution, Anisotropic damage, Plasticity, Microplane model, Nonlinear finite element analysis

Summary. This paper analyzed the propagation of fatigue-induced damage within concrete structures using a microplane fatigue model for concrete, recently created by the authors. Drawing from a recent experimental study that monitored fatigue propagation in prestressed concrete beams, the research provides a comprehensive understanding of the stress redistribution process utilizing the developed model. 3D fatigue simulations of prestressed concrete beams are presented. The numerical studies show that the developed microplane fatigue model is a powerful computational tool for the in-depth analysis of the phenomenon of structural stress redistribution due to compressive fatigue. Furthermore, the model enables the analysis of the the correspondence between the fatigue behavior on the material and structural scales in a wide range of loading configurations.

1 INTRODUCTION

In high-performance reinforced concrete (RC) structures, compressive fatigue in concrete is crucial due to high material utilization, particularly in prestressed, slender structures like wind turbine towers [1, 2, 3]. Over recent decades, significant progress has been made in understanding the fatigue characteristics of concrete. Systematic studies have investigated factors such as loading frequency, temperature e.g. [4], moisture content e.g. [5], loading sequence e.g. [6, 7]. These studies commonly use cylindrical specimens to present key findings in S-N curves, crucial for evaluating fatigue lifetime in current design codes [8, 9].

The transition from material-level fatigue characterization to predicting fatigue behavior in RC structures remains a challenge. To bridge this gap, recent studies have systematically investigated compressive fatigue process zones in concrete structures e.g. [10], including monitoring fatigue degradation in prestressed beams using digital image correlation (DIC) [11]. Despite advances in monitoring, a unified theoretical framework linking material and structural fatigue characteristics is lacking. Accurate prediction of fatigue life requires a deeper theoretical understanding and the development of advanced numerical models. Identifying dissipative mechanisms governing fatigue degradation under cyclic loading is essential.

Recent numerical models describing fatigue damage propagation in concrete fall into two groups [12]: those linking fatigue to load cycles and those based on damage mechanics and

plasticity theories using specific strain measurements. Analytical and empirical models have approximated fatigue behavior of concrete over the lifetime e.g. [13], with fatigue creep curves derived from experimental data. Phenomenological approaches using load cycles as damage variables have also been proposed e.g. [14], alongside tensorial models correlating fatigue damage with strain measure [15, 16, 17].

The development of fatigue crack propagation models in concrete has been significantly advanced by introducing cumulative strain as a key fatigue-inducing variable [18]. This model captures the redistribution of triaxial stress due to microcracks in the fatigue process zone, even at subcritical pulsating loads. This feature of microplane theory [19], was used to integrate the fatigue degradation hypothesis [20]. This integration, in the form of a hemispherical state representation, aims to capture triaxial fatigue-induced stress redistribution in concrete under subcritical compressive fatigue loading [21, 22]. The MS1 fatigue model has shown promise in realistically capturing fatigue degradation at the material level [23].

This paper provides new insights into the propagation and failure of compressive fatigue in concrete by: i) validating the rigorously formulated MS1 model at the structural level, ii) reproducing fatigue propagation through compression zones that cause redistribution of structural stresses, and iii) analyzing the correspondence between fatigue life at the material and structural levels.

2 EXPERIMENTALLY OBSERVED COMPRESSIVE FATIGUE PROPAGATION

To study the structural compressive fatigue behavior of concrete, an externally prestressed T-beam was tested in four-point bending (see Fig. 1a). The design aimed to induce maximum compressive stress at the top, leading to compressive fatigue failure propagating downward. The beam was subjected to two vertical loads and externally prestressed using an eccentric normal force (Fig. 1b). This test setup is designed to mimic the stress configuration that occurs in critical zones of slender structures subjected to high, non-uniform compressive stresses, such as in wind turbines. Detailed information on the test setup and concrete properties is available in [11].

To provide comprehensive data for fatigue model validations at the structural level two prestressed beams, denoted B1 and B2, were tested using a detailed monitoring concept. To capture the propagation of compression fatigue and degradation mechanisms, two techniques were used in the constant moment region, as shown in Fig. 1a. These included digital image correlation (DIC) for recording field data and fiber optic sensors (FOS).

The main results of the tested beam (B1), which exhibit a fatigue failure after 11,933 load cycles, are summarized in Fig. 1c. This figure shows the strain development measured using DIC at different heights throughout the entire fatigue lifetime. These DIC measurements illustrate damage in the compression zone and show strain development throughout the fatigue life. They indicate a gradual increase in compressive strains due to fatigue degradation processes. For a more detailed discussion of experimental results using the monitoring concept and automated DIC-based data evaluation, please refer to [11, 24]. The development of the strain profile over the beam cross-section of B2 measured with FOS during the fatigue life is depicted in Fig. 1d. These experimental results provide valuable observations of compressive fatigue propagation, crucial for assessing the ability of the developed model to capture these aspects.

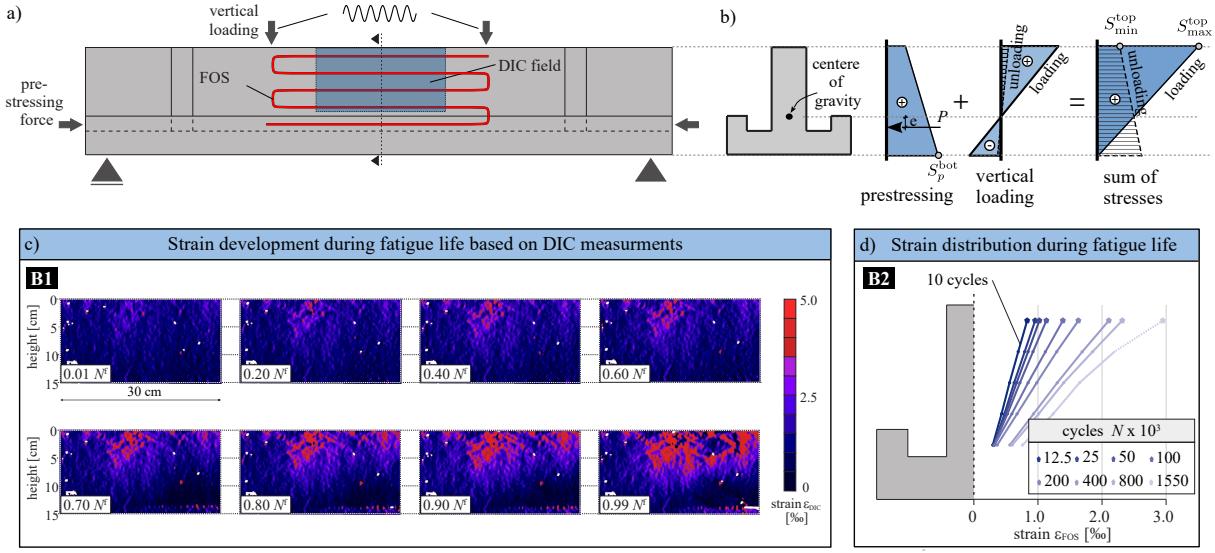

Figure 1: Experimental results from the externally prestressed bending test [11]: a) test setup and measurement techniques used; b) applied forces and the resulting stress profiles across the beam cross-section; c) measured strain field in the central part of beam B1 during the fatigue life using DIC; d) measured strain profile across the cross-section of beam B2 during the fatigue life

3 MICROPLANE SLIDING FATIGUE MODEL MS1

The authors have recently proposed a hypothesis [20, 25, 26] suggesting that concrete fatigue is primarily due to the cumulative effect of sliding damage in the inter-aggregate regions of the material. This is supported by experimental findings presented in [27, 28], which show crack initiation and progression along the interfaces between cement paste and aggregates during fatigue loading. Building on this hypothesis, the authors developed the microplane material model MS1 [22, 23]. MS1 centers on the principle that fatigue damage evolution correlates with cumulative inelastic shear strain, within a thermodynamic framework [16]. Originating from microplane theory, this model uses a homogenization approach based on energy equivalence and employs a direct tensorial method to express effective elastic stiffness.

Kinematic constraint: The strain components projected onto the microplanes, i.e., the normal strain ε_{N} and the tangential strain vector $\boldsymbol{\varepsilon}_{\mathbf{T}}$, are expressed as follows:

$$\varepsilon_{\mathrm{N}} = \boldsymbol{N} : \boldsymbol{\varepsilon}, \quad \boldsymbol{\varepsilon}_{\mathbf{T}} = \boldsymbol{T} : \boldsymbol{\varepsilon}, \tag{1}$$

Here, $\boldsymbol{N}$ is a rank two tensor and $\boldsymbol{T}$ is a rank three tensor obtained as:

$$\boldsymbol{N} = \boldsymbol{n} \otimes \boldsymbol{n}, \qquad \boldsymbol{T} = \boldsymbol{n} \cdot \mathbb{I}_{\mathrm{sym}} - \boldsymbol{n} \otimes \boldsymbol{n} \otimes \boldsymbol{n}, \tag{2}$$

where $\boldsymbol{n}$ represents the normal vector of each microplane, and $\mathbb{I}_{\mathrm{sym}}$ is the symmetric part of the rank four identity tensor.

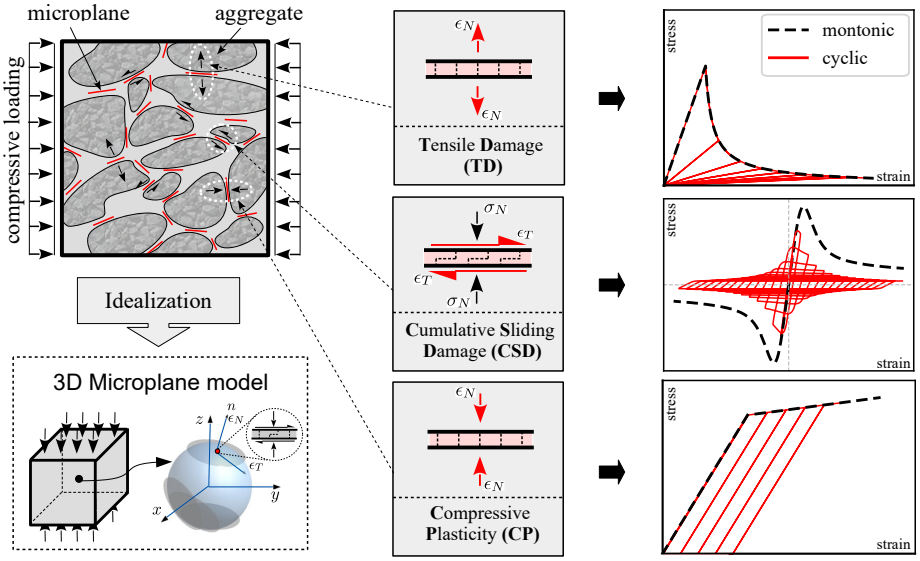

Figure 2: Dissipative mechanisms incorporated within MS1 microplane fatigue model and representation of the microstructure with a system of dissipative microplanes idealized a 3D hemisphere

Microplane constitutive laws: The macroscopic thermodynamic potential is expressed as the sum of the normal and tangential Helmholtz free energies:

$$\psi^{\mathrm{mac}} = \frac{3}{2\pi}\int_{\Omega}\psi^{\mathrm{mic}}\mathrm{d}\Omega = \frac{3}{2\pi}\int_{\Omega}\psi_{\mathrm{N}}^{\mathrm{mic}}\mathrm{d}\Omega + \frac{3}{2\pi}\int_{\Omega}\psi_{\mathrm{T}}^{\mathrm{mic}}\mathrm{d}\Omega. \tag{3}$$

The thermodynamic potentials are projected onto the normal and tangential direction, introducing distinguished dissipative mechanisms for each direction (Fig. 2). The thermodynamically-based constitutive laws at the microplane level for the normal and tangential directions are described in detail in [22]. It is noteworthy that the cumulative tangential damage is identified as the principal factor leading to fatigue damage, resulting in material degradation under subcritical loading conditions.

Homogenization: The homogenization concept, which relies on the principle of energy equivalence, facilitates the mapping between the apparent strain and stress tensors, as detailed in [29]. This approach yields the macroscopic stress in the form of a tensorial constitutive law as

$$\boldsymbol{\sigma} = \boldsymbol{\beta} : \boldsymbol{C}^{\mathrm{e}} : \boldsymbol{\beta}^{\mathrm{T}} : (\boldsymbol{\varepsilon} - \boldsymbol{\varepsilon}^{\mathrm{p}}). \tag{4}$$

To obtain the rank four integrity tensor $\boldsymbol{\beta}$, which represents the 3D damage state, the normal and tangential microplane damage parameters are integrated according to [29] as follows:

$$\begin{aligned}\boldsymbol{\beta}_{ijkl} = &\frac{3}{2\pi}\int_{\Omega}\beta_{\mathrm{N}}^{\mathrm{mic}}\, n_i\, n_j\, n_k\, n_l\, d\Omega \\ &+ \frac{3}{2\pi}\int_{\Omega}\frac{\beta_{\mathrm{T}}^{\mathrm{mic}}}{4}(n_i\, n_k\delta_{jl} + n_i\, n_l\delta_{jk} + n_j\, n_k\delta_{il} + n_j\, n_l\delta_{ik} - 4n_i\, n_j\, n_k\, n_l)\, d\Omega,\end{aligned} \tag{5}$$

The integrity parameter of the normal direction is defined as $\beta_{\mathrm{N}}^{\mathrm{mic}} = \sqrt{1-\omega_{\mathrm{N}}^{\mathrm{mic}}}$, while the integrity parameter of the tangential direction is defined as $\beta_{\mathrm{T}}^{\mathrm{mic}} = \sqrt{1-\omega_{\mathrm{T}}^{\mathrm{mic}}}$. The elastic stiffness tensor, denoted as $\boldsymbol{C}_{ijkl}^{\mathrm{e}}$, can be expressed as:

$$\boldsymbol{C}_{ijkl}^{\mathrm{e}} = \lambda\,\delta_{ij}\delta_{kl} + \mu\,(\delta_{ik}\delta_{jl} + \delta_{il}\delta_{jk}), \tag{6}$$

here, λ and μ are the Lamé parameters. After integrating the normal and tangential microplane plastic strain components, namely $\varepsilon_{\mathrm{N}}^{\mathrm{p,mic}}$ and $\varepsilon_{\mathrm{T}}^{\pi,\mathrm{mic}}$, the rank two macroscopic plastic tensor $\varepsilon_{ij}^{\mathrm{p}}$ can be expressed in 3D as described in [29], following the form:

$$\varepsilon_{ij}^{\mathrm{p}} = \frac{3}{2\pi}\int_{\Omega}\varepsilon_{\mathrm{N}}^{\mathrm{p,mic}} n_i n_j \,\mathrm{d}\Omega + \frac{3}{2\pi}\int_{\Omega}\frac{\varepsilon_{\mathrm{T}r}^{\pi,\mathrm{mic}}}{2}(n_i\delta_{rj} + n_j\delta_{ri})\,\mathrm{d}\Omega. \tag{7}$$

4 FATIGUE SIMULATION OF THE PRESTRESSED BENDING TEST

The developed and validated microplane fatigue model MS1 has been implemented into the finite element software ATENA [30, 31]. This section demonstrates the capability of MS1 model to reproduce fatigue-induced damage propagation at the structural level. The fatigue response of a prestressed bending test setup described in Sec. 3 has been simulated to evaluate this capability. The forthcoming subsections delve into the characteristic aspects of the simulated prestressed bending test under fatigue loading, highlighting the structural behavior and exploring the progression of the fatigue zone and cross-sectional stress redistribution in detail.

To minimize computational cost in the fatigue simulation, three measures were implemented for the initial boundary value problem. Only a quarter of the beam was modeled by utilizing symmetry planes (Fig. 3a). Load levels were intentionally set higher than those used in the experiments to induce fatigue failure within a moderate number of cycles, balancing computational efficiency and aligning with the primary objective of the study to evaluate the ability of the model to replicate fatigue progression and stress redistribution. The middle region of the beam span, where damage localization in the compression zone is expected, was modeled as a nonlinear material using the MS1 fatigue model, while the remaining section was modeled as elastic. The beam has been discretized using 3D tetrahedral elements, each with a size of 0.03m, resulting in a total of 4598 elements.

In line with the prestressed bending tests explained in section 2, a prestressing force of 618 kN was applied, resulting in a stress level of $S_{\mathrm{p}}^{\mathrm{bot}} = 0.54\ f_{\mathrm{c}}$ at the bottom fiber of the mid-span section. The calibrated model parameters described in [30] for concrete with a compressive strength of $f_{\mathrm{c}} = 48.75$ MPa were used. For the fatigue loading, the upper and lower load levels were set at $F_{\max} = 219.6$ kN and $F_{\min} = 9.8$ kN, respectively. These levels correspond to the maximum and minimum stress levels at the top fiber in the mid-span section during loading and unloading, quantified as $S_{\max}^{\mathrm{bot}} = 0.966\ f_{\mathrm{c}}$ and $S_{\min}^{\mathrm{bot}} = 0.04\ f_{\mathrm{c}}$.

The simulated load-deflection response under fatigue loading is shown in Fig. 3b, representing the complete loading history. The beam experienced fatigue failure after 405 loading cycles. To better illustrate the shape of hysteretic loops, several load cycles, including the first cycle, cycle 200, and the last cycle (cycle 405), are presented in Fig. 3c. These cycles show a plausible form of hysteretic loops. The corresponding fatigue creep curve, which illustrates the increase in deformation during the fatigue life at the upper load level, is shown in Fig. 3d. The curve has a realistic shape as observed in fatigue tests, with a rapid deformation growth in the initial

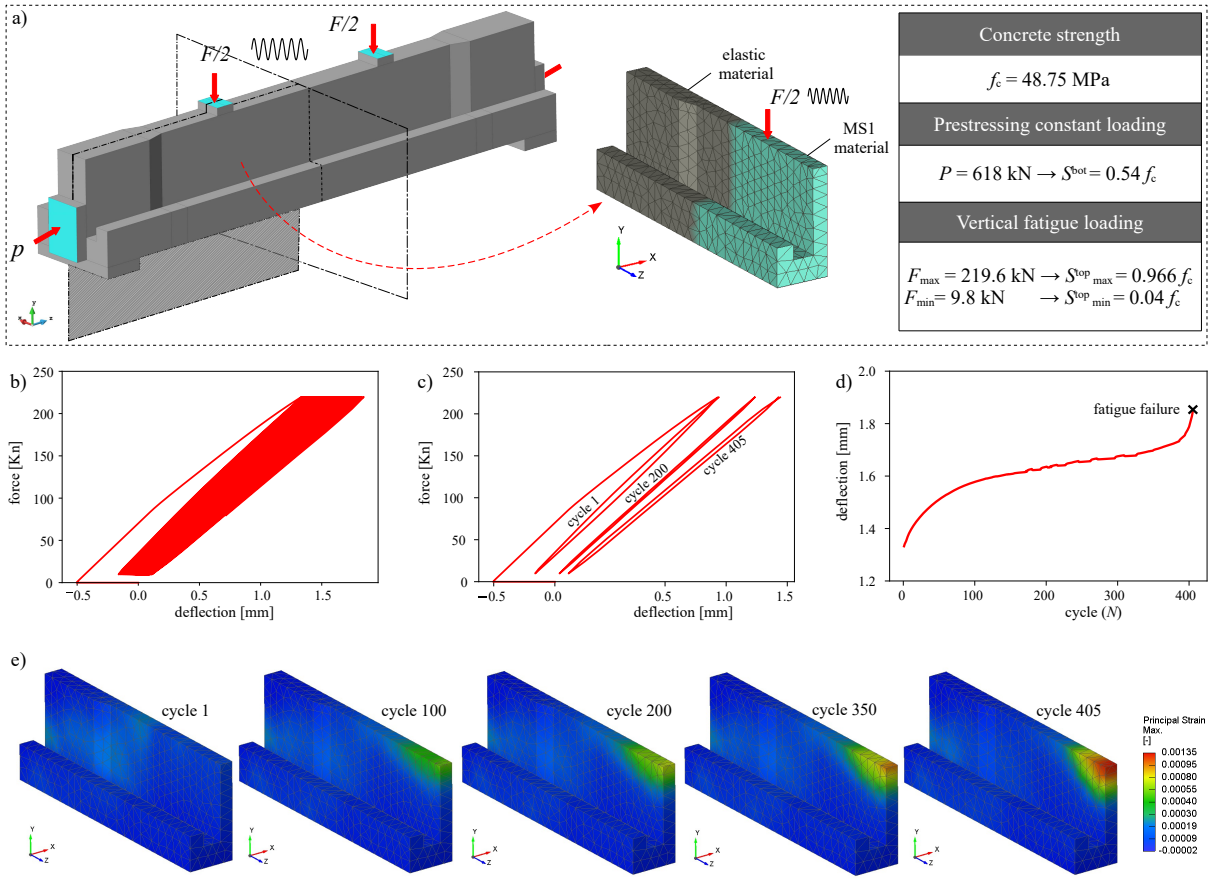

Figure 3: Simulation of an externally prestressed bending test: a) 3D sketch of the beam with the applied forces and compressive behavior of a single material point; b) load-deflection response under fatigue loading; c) load-deflection response of three selected loading cycles; d) corresponding fatigue creep curve; e) compression-fatigue propagation visualized based on the maximum principal strains for selected loading cycles

and final phases and an almost linear, moderate deformation growth in the intermediate phase. In particular, the model accurately captures the shape of the first branch of the fatigue creep curve, which shows a decreasing rate of inelastic deformation as a structural effect.

To illustrate the localization leading to fatigue failure, contour plots of the maximum principal strain are presented for the simulated quarter of the beam at eight stages during fatigue loading, as shown in Fig. 3e. The contour plots indicate clearly the development and propagation of compression fatigue, especially in the upper and middle regions of the beam. This observation agrees well with the experimental results of beam B1, which were recorded with DIC measurements (see Fig. 1c). The comparison of the contour plots with the experimental data shows that the model accurately reflects the qualitative behavior of compressive fatigue in concrete members.

The development of the strains along the cross-section in the mid-span is shown in Fig. 4a. The black strain profiles represent the loading conditions immediately after prestressing as well as the lower and mean values of the first load cycle. The increase in strain during the fatigue

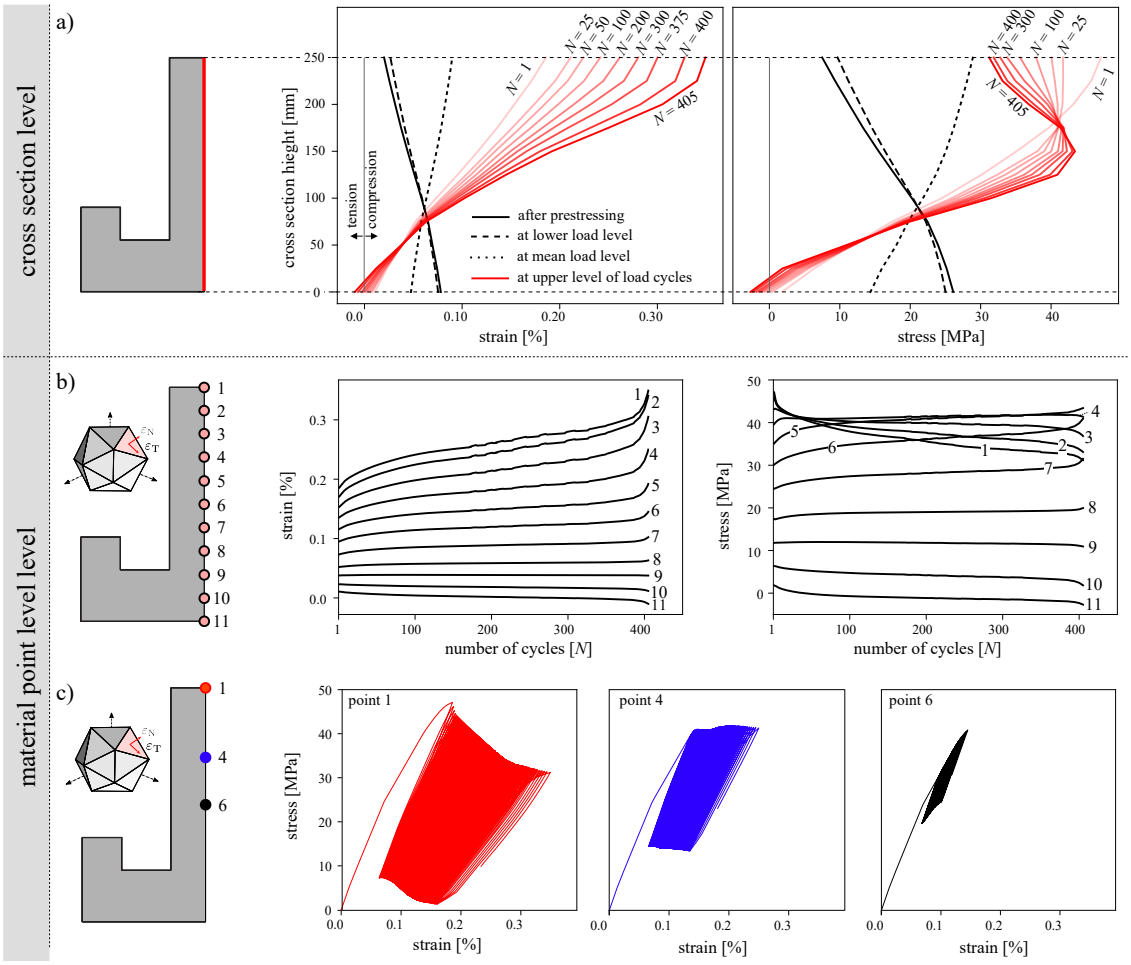

Figure 4: Strain and stress development in the simulated prestressed bending test: a) strain and stress profiles across the mid-span cross-section for selected loading cycles b) strain and stress development during the fatigue life, determined for several points across the mid-span cross-section c) cyclic stress-strain histories of selected three points along the mid-span cross-section

life can be seen from the red profiles plotted for selected load cycles. These results are in good qualitative agreement with the observed experimental results of B2 during the fatigue life, as shown in Fig. 1d. The numerically determined stress profiles are shown in Fig. 4a. The change in the stress profiles during the fatigue life illustrates a remarkable phenomenon of stress redistribution at the structural level. Comparing the stress profile at the first and last loading cycle, this effect becomes evident as the stresses at the top fiber decrease due to fatigue-induced deterioration, while at the same time they increase over the middle part of the cross-section, as shown in Fig. 4a.

Fig. 4b illustrates the strain and stress curves for individual points across the height of the mid-span cross-section. These curves represent the stress and strain profiles over the entire fatigue life at maximum load. The typical S-shape of the fatigue creep [32] curve can be reproduced reasonably well, as shown in Fig. 4b for points 1-7. The stress curves obtained show that the fatigue degradation occurs predominantly in the upper part of the cross-section, especially

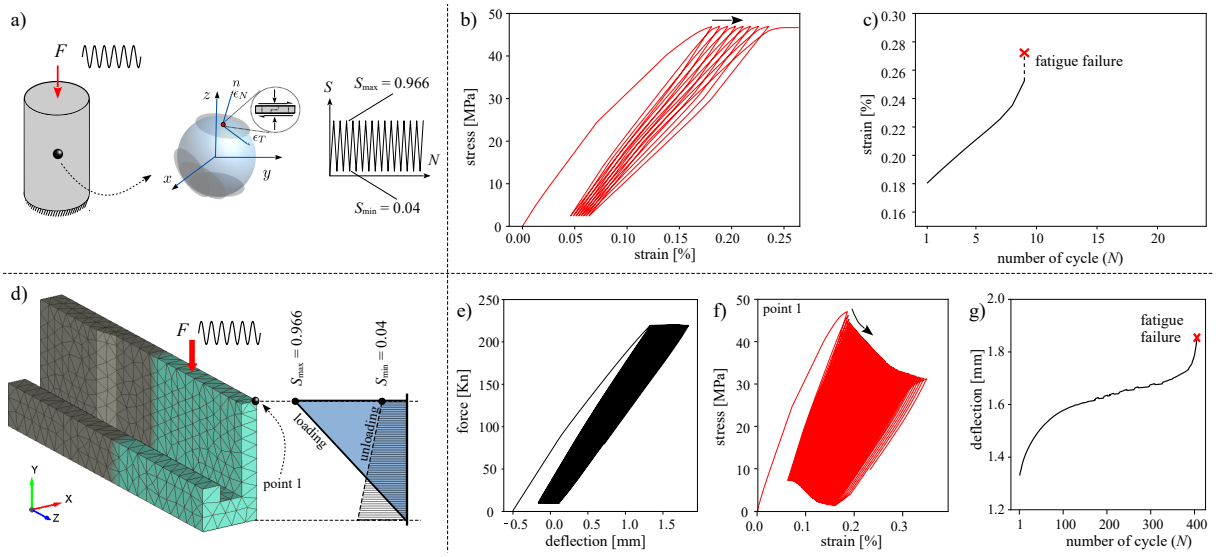

Figure 5: Material vs. structural fatigue behavior: a) Idealization of a single material point with the applied load range; b) cyclic stress-strain response; c) corresponding fatigue creep curve; d) 3D beam with applied load range; e) cyclic load-deflection response; f) experienced stress-strain response at point 1; g) corresponding fatigue creep curve

from point 1 to point 4. In contrast, the stresses at the other points of the cross-section have either increased or remained relatively unchanged.

The cyclic stress-strain response of selected points along the cross-section is shown in Fig. 4c. These curves clearly show that each material point is subject to a non-uniform loading scenario due to the fatigue of some points and the resulting stress redistribution at the structural level. Furthermore, the structural stress redistribution process allows a reduction of the applied stress in the most critical areas, e.g. point 1 and point 2 (Fig. 4c), which in turn leads to a significant extension of the fatigue life at these specific points. This observation underlines the importance of studying the fatigue behavior of concrete not only under constant stress amplitudes, but also considering variable amplitudes [33, 34, 35]. In this context, it is worth mentioning that variable amplitudes of fatigue loading are not only the result of stochastic loading scenarios, as usually assumed, but also occur due to the aforementioned process of structural stress redistribution

5 MATERIAL FATIGUE LIFE VS. STRUCTURAL FATIGUE LIFE

The fatigue modeling framework presented here provides a tool that can be used to improve the understanding of concrete fatigue at a structural level and shows how fatigue-induced stress redistribution affects the service life of structures. Currently design codes do not take this effect into account. Fig. 5 compares the fatigue life predictions with and without stress redistributions. The current method for fatigue life assessment according to the Eurocodes, which is represented by a simulation with a single material point (Fig. 5a), uses upper and lower load levels based on elastic stress values in the upper fiber mid-section of the beam (Fig. 5d). This corresponds to typical compression fatigue tests on cylindrical concrete specimens.

The cyclic stress-strain behavior of the material point simulation is shown in Fig. reffig b. The structural response of the prestressed beam is shown in the load-deflection plot (Fig. 5e),

and the local stress-strain response at point 1 is shown in Fig. 5f. Corresponding fatigue creep curves are shown in Fig. 5c and Fig. 5g.

The material point simulation, using the same stress levels as for the upper cross-section point, predicts failure after 8 load cycles, which is close to the fib Model Code 2010 [8] prediction of 4 cycles. Conversely, as shown in Fig. 5c, the simulated beam fails after 405 load cycles. This comparison shows that the fatigue life of a prestressed beam on the structural scale significantly exceeds the fatigue life on the material scale due to the redistribution of stresses. This redistribution gradually reduces the fatigue stresses in the critical zones, significantly increasing their fatigue life and that of the entire component. These results are consistent with experimental evidence showing that prestressed concrete beams have a much longer fatigue life than estimated in the fib Model Code 2010 as documented in [36].

These observations, along with our numerical analyses, suggest that current fatigue assessment methods, which ignore stress redistribution, may be overly conservative. However, this conclusion needs further examination across various structural configurations. The MS1 fatigue model, which considers key fatigue-induced dissipative mechanisms and stress redistribution effects, can be instrumental in this regard. It offers a robust framework to link fatigue properties identified in material characterization tests with the fatigue response of typical reinforced concrete members. Further corresponding studies on the evaluation and analysis of energy dissipation during fatigue life are presented in [37].

It is crucial to emphasize that the ultimate objective is to predict the fatigue behavior of reinforced concrete structures. To streamline complexity, this study deliberately focuses on analyzing the propagation of compressive fatigue in a plain concrete zone. The MS1 fatigue model employed here is well-suited for ongoing investigations into the fatigue behavior of reinforced concrete members. Additionally, to address bond deterioration under fatigue loading, researchers can utilize a recently developed bond fatigue model by the authors [26], which also incorporates interactions between bond fatigue and the splitting effect around the reinforcement.

6 CONCLUSIONS

The presented MS1 microplane fatigue model offers the capability to study the structural fatigue characteristics of concrete members. This model accurately captures the progression of compressive fatigue and effectively simulates the stress redistribution phenomenon associated with structural fatigue, as demonstrated in an externally prestressed bending beam.

The numerical results reveal a significant discrepancy between the fatigue lifetimes at the structural and material scales. This contrast underscores the critical importance of understanding the correspondence between material and structural fatigue responses across a wider range of configurations. Characterizing this correspondence is a key objective for future research aimed at providing realistic predictions of the fatigue life of reinforced concrete structures.

Acknowledgment

The work was supported by the German Research Foundation (DFG) in the framework of the joint project (EnFatiCon: Energy dissipation-based approach to stochastic fatigue of concrete considering interacting time and temperature effects), project number (471796896). This support is gratefully acknowledged.

REFERENCES

[1] B. Schmidt, S. Schneider, S. Marx, Concrete fatigue-safety and development potential of current design concepts, Bautechnik 96 (4) (2019) 329–337.

[2] A. Baktheer, C. Goralski, J. Hegger, R. Chudoba, Stress configuration-based classification of current research on fatigue of reinforced and prestressed concrete, Structural Concrete (2024). doi:10.1002/suco.202300667.

[3] H. Becks, M. Aguilar, A. Baktheer, R. Chudoba, M. Classen, Experimental and numerical investigations on the fatigue behavior of high-strength concrete under combined shear-compression loading, IABSE Proceedings of IABSE symposium: challenges for existing and oncoming structures, Prague, Czech Republic (2022) 532–540.

[4] K. Elsmeier, J. Hümme, N. Oneschkow, L. Lohaus, Prüftechnische Einflüsse auf das Ermüdungsverhalten hochfester feinkörniger Vergussbetone, Beton- und Stahlbetonbau 111 (4) (2016) 233–240. doi:10.1002/best.201500065.

[5] C. Tomann, N. Oneschkow, Influence of moisture content in the microstructure on the fatigue deterioration of high-strength concrete, Structural Concrete 20 (4) (2019) 1204–1211. doi:10.1002/suco.201900023.

[6] J. O. Holmen, Fatigue of concrete by constant and variable amplitude loading, ACI Journal, Special Publication 75 (1982) 71–110. doi:10.14359/6402.

[7] A. Baktheer, R. Chudoba, Experimental and theoretical evidence for the load sequence effect in the compressive fatigue behavior of concrete, Materials and Structures 54 (2) (2021) 82. doi:10.1617/s11527-021-01667-0.

[8] fib Model Code 2010, International Federation for Structural Concrete, fib model code for concrete structures (Model Code 2010). doi:10.1002/9783433604090.

[9] EN-1992-2, Eurocode 2: Design of concrete structures, Part 2: Concrete bridges - Design and detailing rules, European Committee for Standardisation, 2005.

[10] D. Birkner, R. E. Beltrán Gutiérrez, S. Marx, Comparison of stiffness degradation in fatigue-loaded concrete cylinders and large-scale beams, Engineering Structures 302 (2024) 117360. doi:10.1016/j.engstruct.2023.117360.

[11] H. Becks, A. Baktheer, S. Marx, M. Classen, J. Hegger, R. Chudoba, Monitoring concept for the propagation of compressive fatigue in externally prestressed concrete beams using digital image correlation and fiber optic sensors, Fatigue & Fracture of Engineering Materials & Structures 46 (2) (2023) 514–526. doi:10.1111/ffe.13881.

[12] A. Baktheer, R. Chudoba, Classification and evaluation of phenomenological numerical models for concrete fatigue behavior under compression, Construction and Building Materials 221 (2019) 661 – 677. doi:10.1016/j.conbuildmat.2019.06.022.

[13] M. Jia, Z. Wu, H. Wang, R. C. Yu, X. Zhang, Analytical method for predicting mode i crack propagation process of concrete under low-cycle fatigue loading, Engineering Fracture Mechanics 286 (2023) 109320. doi:10.1016/j.engfracmech.2023.109320.

[14] D. Pfanner, Zur Degradation von Stahlbetonbauteilen unter Ermüdungsbeanspruchung, Ph.D. thesis, Ruhr-Universität Bochum, Bochum, Germany: (2003).

[15] A. Alliche, Damage model for fatigue loading of concrete, International Journal of Fatigue 26 (9) (2004) 915–921. doi:10.1016/j.ijfatigue.2004.02.006.

[16] R. Desmorat, F. Ragueneau, H. Pham, Continuum damage mechanics for hysteresis and fatigue of quasi-brittle materials and structures, International Journal for Numerical and Analytical Methods in Geomechanics 31 (2) (2007) 307–329. doi:10.1002/nag.532.

[17] A. Baktheer, E. Martínez-Pañeda, F. Aldakheel, Phase field cohesive zone modeling for fatigue crack propagation in quasi-brittle materials, Computer Methods in Applied Mechanics and Engineering (2024) 116834doi:10.1016/j.cma.2024.116834.

[18] K. Kirane, Z. P. Bažant, Microplane damage model for fatigue of quasibrittle materials: Sub-critical crack growth, lifetime and residual strength, International Journal of Fatigue 70 (2015) 93–105. doi:10.1016/j.ijfatigue.2014.08.012.

[19] Z. P. Bažant, B. Oh, Microplane model for fracture analysis of concrete structures, Proceedings of the Symposium on the Interaction of Non-Nuclear Munitions with Structures, 1983, pp. 49–55.

[20] A. Baktheer, R. Chudoba, Pressure-sensitive bond fatigue model with damage evolution driven by cumulative slip: Thermodynamic formulation and applications to steel- and frp-concrete bond, International Journal of Fatigue 113 (2018) 277 – 289. doi:10.1016/j.ijfatigue.2018.04.020.

[21] A. Baktheer, M. Aguilar, J. Hegger, R. Chudoba, Microplane damage plastic model for plain concrete subjected to compressive fatigue loading, 10th International Conference on Fracture Mechanics of Concrete and Concrete Structures, FraMCoS-X, 2019. doi:10.21012/FC10.233196.

[22] A. Baktheer, M. Aguilar, R. Chudoba, Microplane fatigue model MS1 for plain concrete under compression with damage evolution driven by cumulative inelastic shear strain, International Journal of Plasticity 143 (2021). doi:10.1016/j.ijplas.2021.102950.

[23] M. Aguilar, A. Baktheer, R. Chudoba, Numerical investigation of load sequence effect and energy dissipation in concrete due to compressive fatigue loading using the new microplane fatigue model MS1, Onate, E., Peric, D., Chiumenti, M., de Souza Neto, E., Eds; COMPLAS 2021; Barcelona, Spain, 2021. doi:10.23967/complas.2021.053.

[24] F. Seemab, M. Schmidt, A. Baktheer, M. Classen, R. Chudoba, Automated detection of propagating cracks in rc beams without shear reinforcement based on dic-controlled modeling of damage localization, Engineering Structures 286 (2023) 116118. doi:10.1016/j.engstruct.2023.116118.

[25] A. Baktheer, R. Chudoba, Modeling of bond fatigue in reinforced concrete based on cumulative measure of slip, in: Computational Modelling of Concrete Structures, EURO-C 2018, CRC Press, 2018, pp. 767–776. doi:10.1201/9781315182964-90.

[26] R. Chudoba, M. Vořechovský, M. Aguilar, A. Baktheer, Coupled sliding–decohesion–compression model for a consistent description of monotonic and fatigue behavior of material interfaces, Computer Methods in Applied Mechanics and Engineering 398 (2022) 115259. doi:10.1016/j.cma.2022.115259.

[27] L. Skarzynski, I. Marzec, J. Tejchman, Fracture evolution in concrete compressive fatigue experiments based on x-ray micro-ct images, International Journal of Fatigue 122 (2019) 256–272. doi:10.1016/j.ijfatigue.2019.02.002.

[28] S. Rybczynski, G. Schaan, M. Dosta, M. Ritter, F. Schmidt-Döhl, Discrete element modeling and electron microscopy investigation of fatigue-induced microstructural changes in ultra-high-performance concrete, Materials 14 (21) (2021). doi:10.3390/ma14216337.

[29] I. Carol, Z. P. Bažant, Damage and plasticity in microplane theory, International Journal of Solids and Structures 34 (29) (1997) 3807–3835. doi:10.1016/S0020-7683(96)00238-7.

[30] M. Aguilar, A. Baktheer, R. Chudoba, On the energy dissipation in confined concrete subjected to shear cyclic loading, Proceedings in Applied Mathematics and Mechanics 22 (1) (2023) e202200301. doi:10.1002/pamm.202200301.

[31] V. Cervenka, J. Cervenka, R. Pukl, Atena—a tool for engineering analysis of fracture in concrete, Sadhana 27 (4) (2002) 485–492. doi:10.1007/BF02706996.

[32] A. Baktheer, H. Spartali, R. Chudoba, J. Hegger, Concrete splitting and tip-bearing effect in the bond of anchored bars tested under fatigue loading in the push-in mode: An experimental investigation, Materials and Structures 55 (3) (2022) 101. doi:10.1617/s11527-022-01935-7.

[33] A. Baktheer, J. Hegger, R. Chudoba, Enhanced assessment rule for concrete fatigue under compression considering the nonlinear effect of loading sequence, International Journal of Fatigue 126 (2019) 130 – 142. doi:10.1016/j.ijfatigue.2019.04.027.

[34] A. Baktheer, H. Becks, Fracture mechanics based interpretation of the load sequence effect in the flexural fatigue behavior of concrete using digital image correlation, Construction and Building Materials 307 (2021). doi:10.1016/j.conbuildmat.2021.124817.

[35] A. Baktheer, B. Camps, J. Hegger, R. Chudoba, Numerical and experimental investigations of concrete fatigue behavior exposed to varying loading ranges, The 5th International fib Congress, 2018, p. 14.

[36] D. Birkner, S. Marx, Stiffness degradation in fatigue loaded large concrete beams, in: 6th fib International Congress on Concrete Innovation for Sustainability, The International Federation for Structural Concrete (fib), 2022, pp. 2008–2017.

[37] A. Baktheer, S. Esfandiari, M. Aguilar, H. Becks, M. Classen, R. Chudoba, Fatigue-induced stress redistribution in prestressed concrete beams modeled using the constitutive hypothesis of inter-aggregate degradation, Fatigue & Fracture of Engineering Materials & Structures (2024). doi:10.1111/ffe.14388.